MR Imaging of the hip: Avoiding pitfalls, identifying normal variants

Brian Y. Chan, MD; Hailey Allen, MD; Kirkland W. Davis, MD, FACR; and Donna G. Blankenbaker, MD

The hip is a complex ball-and-socket joint comprising the acetabulum, proximal femur, and articular cartilage. In addition, the capsulolabral tissues and surrounding muscles and tendons stabilize the hip, dictate its range of motion, and enhance its function. Familiarity with the spectrum of magnetic resonance imaging (MRI) appearances of the hip is necessary to recognize normal variants and distinguish them from true pathologic conditions.

This article provides a brief overview of considerations in tailoring protocols of the bony pelvis and hip to optimize detection of both intra- and extra-articular hip pathology, followed by a review of common labral, osteocartilaginous, and soft tissue variants that can be mistaken for true pathology.

Dr. Chan and Dr. Allen are Radiologists at the University of Utah School of Medicine, Salt Lake City, UT; and Dr. Davis and Dr. Blankenbaker are Radiologists at the University of Wisconsin School of Medicine and Public Health, Madison, WI. Dr. Blankenbaker and Dr. Davis are Consultants for and receive royalties from Elsevier.

Imaging protocol

Dedicated MRI protocols for imaging the pelvis and hip vary among institutions, but there are key elements common to most. In patients with nonspecific hip pain, even unilateral symptoms, large field-of-view (FOV) images of the pelvis (30 cm or more) are commonly performed, spanning the region from the iliac crests to the level of the lesser trochanters. This prevents other pelvis pathology that can mimic hip pain from being overlooked. Coronal T1-weighted images without fat suppression are best for revealing detailed anatomy and evaluating bone marrow and musculature. Large FOV fluid-sensitive sequences, either T2-weighted with fat suppression or short tau inversion recovery (STIR), are obtained in the coronal and axial planes and are used to evaluate for fractures, fluid collections, and injuries involving tendon or muscle. Larger slice thicknesses (5-7 mm) with small interslice gaps can be permitted for these large FOV images. For pelvic imaging, depending on patient body size, either a torso phased array coil or a larger body coil can be used. Depending on the referring clinician, dedicated imaging of the symptomatic hip may be performed only based on the clinical examination and clinical question.

Dedicated imaging of the symptomatic hip should be performed using a surface coil, such as a cardiac phased array coil, with the smallest possible FOV (15-20 cm) extending from the top of the anterior inferior iliac spine to the bottom of the lesser trochanter. Small-FOV images with fluid-sensitive sequences (proton density [PD] or T2-weighted with fat suppression) provide the best evaluation of the acetabular labrum and articular cartilage on non-arthrographic examinations. Small slice thickness (2-3.5 mm) with minimal or no interslice gap is important for these acquisitions. Plane selection in hip imaging is challenging, as the hip joint is

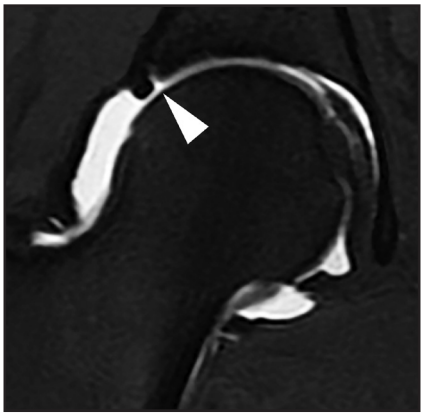

FIGURE 1. *Sublabral sulcus. Coronal T1-weighted fat-suppressed MR arthrogram image of the right hip in a 19-year-old woman shows a thin, smooth, linear extension of intra-articular contrast at the superior chondrolabral junction (arrowhead). The typical location, depth, smooth margins and absence of signal abnormality in the adjacent labrum helps to distinguish this variation from a labral tear.*

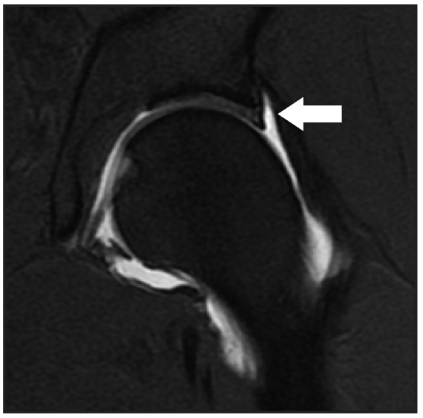

FIGURE 2. *Perilabral recess. Coronal T2-weighted fat-suppressed MR arthrogram image in a 51-year-old man demonstrates fluid signal interposed between the labrum and the joint capsule (arrow). Note that the superior insertion of the joint capsule is several millimeters above the acetabular roof.*

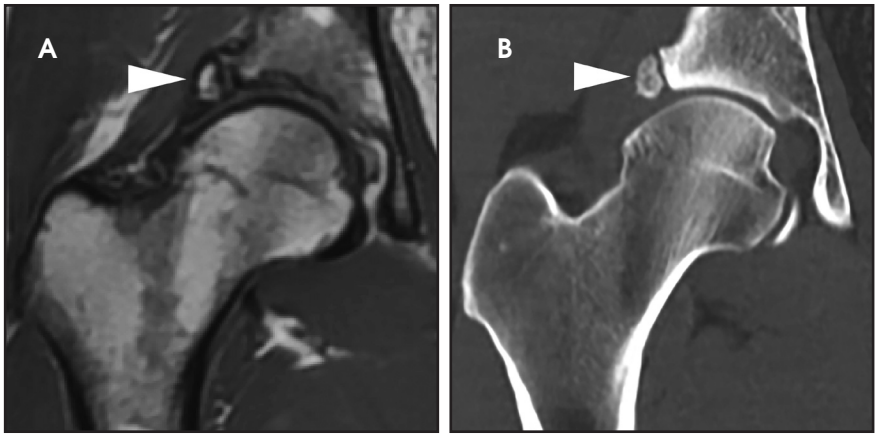

FIGURE 3. *Os acetabuli. Coronal T1-weighted MR image (A) in a 28-year-old man demonstrates a rounded structure following marrow signal intensity (arrowhead), which is separate from the adjacent acetabulum. Coronal CT image (B) from the same patient demonstrates that the structure identified on MR corresponds to a well-corticated ossicle (arrowhead).*

a highly curved structure with closely opposed cortical surfaces and relatively thin articular cartilage, making it particularly susceptible to partial volume averaging.[1] Traditional (axial, sagittal, and coronal) planes are used, as are off-axis planes (oblique axial and oblique sagittal). Routine radial imaging to assess labral and femoral head morphology can be performed to visualize multiple segments of the labrum and articular cartilage in cross section.[2] For MR arthrography, multiplanar small-FOV images with T1- and T2-weighting, both with fat suppression, help to delineate fluid- or contrast-filled clefts in the labrum or cartilage and paralabral cysts. Indirect MR arthrography, which entails imaging after administering intravenous gadolinium followed by exercising the extremity of interest, has been reported accurate in labral tear detection and is utilized in some centers.[3,4] MR arthrography can be helpful to the surgeon, as anesthetic is administered as part of the injectate; this can provide additional information on pain relief and has been found to be 90% accurate in those with intra-articular pathology in at least one study.[5]

Conventional MRI and MR arthrography are both excellent detectors of extra-articular pathology of the hip, whereas the latter has been shown superior in detecting intra-articular pathology, particularly labral tears. Meta-analysis data suggest pooled sensitivity and specificity of 66% and 79%, respectively, for conventional MRI in detecting labral tears, compared to 87%–97% and 64% for MR arthrography.[6,7] MR arthrography is also superior for evaluating the articular cartilage, with sensitivities ranges of 71-92% compared to 58–83% for conventional MRI.[8-10] Examinations performed at 3.0T provide higher resolution and greater signal-to-noise compared to those performed at 1.5T, with some data suggesting conventional MRI at 3.0T has similar to slightly higher detection for labral tears than MR arthrography performed at 1.5T.[11] Protocols using 3D acquisitions may potentially reduce scan time without sacrificing diagnostic accuracy. One study of MR arthrography of the hip at 3.0T demonstrated that sensitivity and specificity for labral pathology did not differ significantly between conventional multiplanar 2D acquisitions and a single isotropic 3D sequence reconstructed into multiple planes.[12]

Labral pitfalls

Normal labrum

The labrum is a fibrocartilaginous structure attached to the peripheral acetabulum. It facilitates appropriate acetabular formation during skeletal maturation, stabilizes the femoral head by deepening the acetabulum, and seals synovial fluid within the hip joint. The normal labrum is most frequently triangular in morphology but demonstrates an increasingly rounded and irregular shape in asymptomatic hips with increasing age.[13] The labrum reportedly is absent in 3% of patients.[14] There is also a wide range of normal labral signal characteristics, including intermediate signal intensity on T1-, proton density-, and

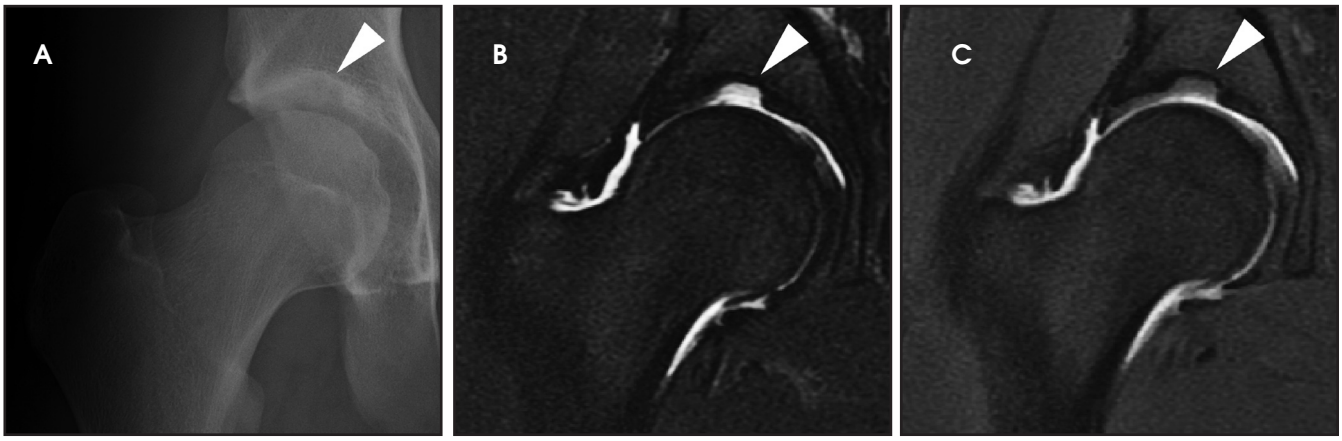

FIGURE 4. *Supraacetabular fossa. Anteroposterior radiograph of the right hip (A) in a 15-year-old boy demonstrates an apparent depression/defect in the articular surface of the right acetabulum at the 12 o'clock position (arrowhead). Coronal T2-weighted fat-suppressed MR arthrogram image (B) shows this to be a defect in the acetabular roof located lateral to the acetabular fossa. Coronal T1-weighted fat-suppressed MR arthrogram image (C) shows that this defect is filled with articular cartilage, suggesting it may be occult at arthroscopy. The classic location, smooth margins, and lack of associated bone marrow edema distinguish the SAF from a pathologic lesion of the articular cartilage or subchondral bone plate.*

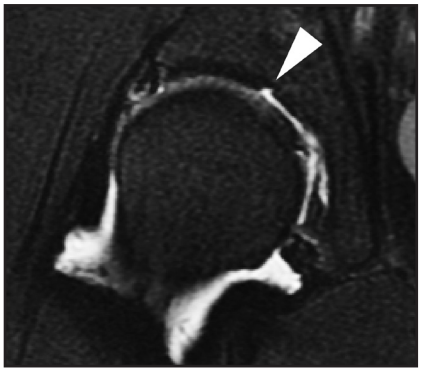

FIGURE 5. *Stellate crease. Coronal T1-weighted fat-suppressed MR arthrogram image in a 23-year-old woman demonstrates a thin fluid-filled defect in the acetabular roof (arrowhead). Note that this is located more medially than expected for a supraacetabular fossa, and there is no associated defect in the underlying bone. The lack of subchondral bone marrow edema or adjacent chondral abnormality helps distinguish the stellate crease from a true cartilage abnormality. Moreover, this would be a very unusual location for an isolated cartilage defect.*

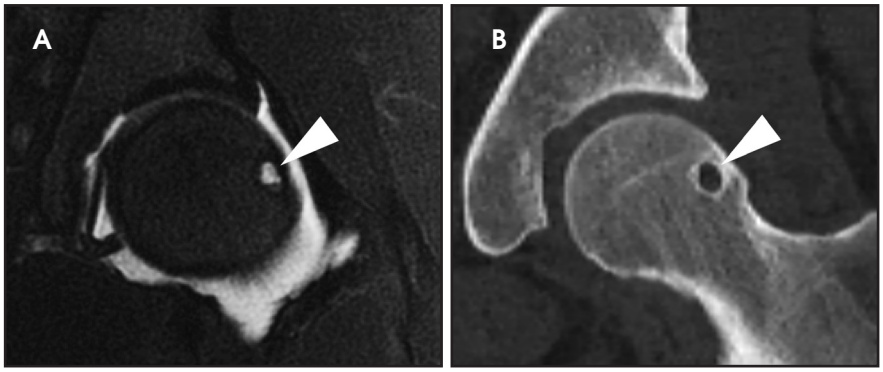

FIGURE 6. *Synovial herniation pit. Coronal T2-weighted fat-suppressed image (A) in a 23-year-old woman demonstrates a small, round hyperintense lesion at the anterior femoral head-neck junction (arrowhead). Noncontrast CT image (B) from the same patient shows a corresponding lucent lesion with a non-aggressive appearing sclerotic rim (arrowhead).*

T2-weighted images and, less commonly, high signal intensity on T2-weighted images.

Diagnostic criteria for labral tears includes the presence of labral distortion, high signal intensity on T2-weighted imaging, or gadolinium contrast extending into the labral substance or acetabular-labral junction. An adjacent paralabral cyst is a useful secondary sign of a labral tear and should increase diagnostic confidence or raise suspicion for a labral tear.[15] The most common location of labral tears is anterosuperior.[16-18]

Sublabral sulcus

Normal labral variants that manifest as high T2-weighted signal in or adjacent to the labrum can be mistaken for a labral tear. One common variant, the sublabral sulcus, is seen in up to 25% of patients.[19] MR imaging characteristics include a linear shape with smooth edges, location at the chondrolabral junction (undermining the labrum rather than extending into it), not full-thickness, and absence of signal changes elsewhere in the labrum (Figure 1). The sublabral sulcus can occur anywhere in the labrum, but it most commonly appears posteroinferiorly (48%) or anterosuperiorly (44%), followed by posterosuperiorly (4%) and anteroinferiorly (4%).[19] Several studies have questioned whether sublabral sulci actually represent partial or partially healed labral tears, including one published by Magerkurth et al, who found no sublabral sulci with either MR arthrography or arthroscopy in a small series of patients younger than 17 years old.[20] In distinguishing between a labral tear and a sulcus, a labral tear should be suspected if the abnormality is located within the anterosuperior aspect of the labrum, accompanied by appropriate clinical history, and intra-articular anesthetic brings pain relief.

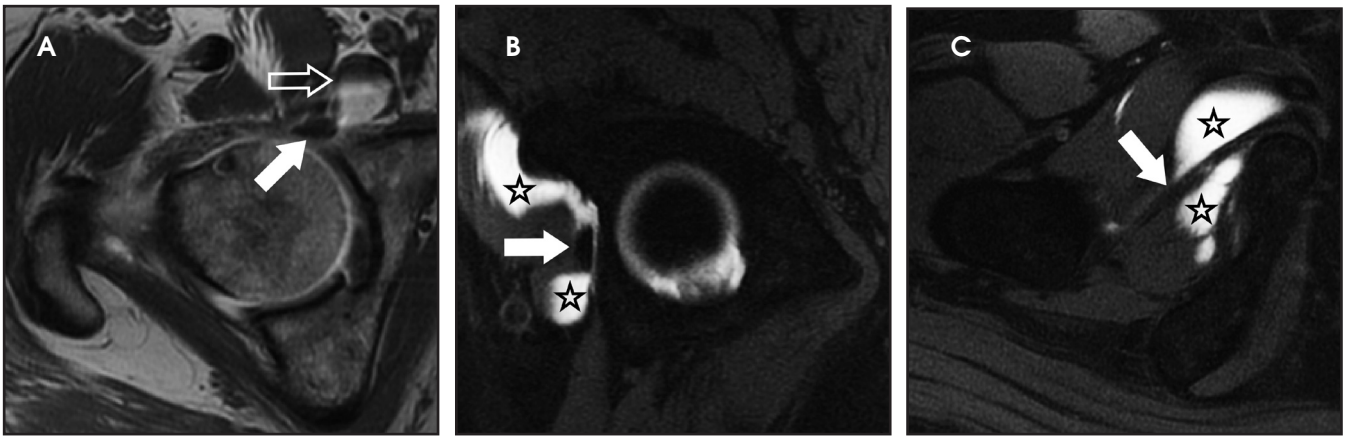

FIGURE 7. *Iliopsoas bursa. Axial T1-weighted MR arthrogram image of the right hip (A) in a 66-year-old woman demonstrates a fluid-gadolinium level (open arrow) next to the iliopsoas tendon (solid arrow), confirming communication of the iliopsoas bursa with the hip joint. T1-weighted fat-suppressed MR arthrogram images in the sagittal (B) and oblique axial (C) planes demonstrate the characteristic appearance of ovoid fluid collections (stars) on either side of the iliopsoas tendon (arrow).*

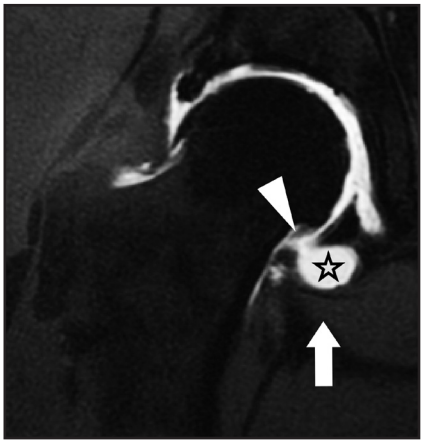

FIGURE 8. *Obturator externus bursa. Coronal T1-weighted fat-suppressed MR arthrogram image (A) in a 59-year-old woman demonstrates rounded, inferomedial extension of gadolinium (star), which communicates with the hip joint via a narrow neck (arrowhead). There is inferior displacement of the obturator externus muscle (arrow). Axial T2-weighted fat-suppressed image (B) demonstrates this same contrast-filled outpouching (star) in the plane of the obturator externus muscle and separate from the hip joint capsule (arrow).*

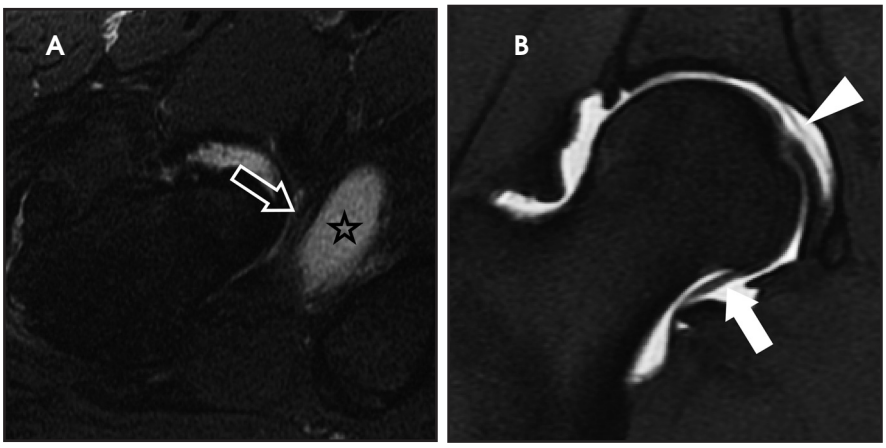

FIGURE 9. *Pectinofoveal fold and ligamentous plica. Coronal T1-weighted fat-suppressed image from an MR arthrogram of the right hip (A) in a 21-year-old woman shows the normal appearance of the pectinofoveal fold as a thin, hypointense curvilinear structure extending from the inferomedial femoral head-neck junction to its inferior attachment onto the inferior joint capsule (arrow). Immediately adjacent to the ligamentum teres is a ligamentous plica seen as a fine, linear, slightly undulating hypointense structure (B, arrowhead) within the joint space.*

Perilabral sulcus

A perilabral sulcus or recess is a normal potential space interposed between the labrum and overlying joint capsule. These are most conspicuous in the superior joint space, where the joint capsule inserts several millimeters superior to the labrum (Figure 2), but they can also be seen along the anterior and posterior joint capsule. Perilabral sulci are easy to detect if the joint is distended with a joint effusion or contrast, as is the case in MR arthrography. However, if the joint is not distended, a small volume of trapped fluid in the perilabral recess may mimic a paralabral cyst.[21] If the perilabral sulcus is large, it may mimic capsular stripping.

Osteocartilaginous pitfalls

Os acetabuli

An os acetabuli is a small accessory ossification center located adjacent to the acetabular rim present in 2-3% of the population.[22] On radiography, they appear as a well-corticated ossicle adjacent to the acetabulum, most common anterosuperiorly. On MRI, these ossicles follow marrow signal intensity and are separated from the acetabulum by a thin cartilage rim (Figure 3). At least one sequence without fat suppression is necessary to discern the typical appearance of marrow within the ossicle and to ensure the ossicle is not confused with a labral tear. When located in the acetabular fossa (os acetabuli centrale), they may mimic an intra-articular body.[23] Os acetabuli can also be acquired as sequelae of incompletely healed fractures or ossification of the acetabular labrum. These structures are typically asymptomatic; if large enough, however, they may contribute to symptoms of femoroacetabular impingement.

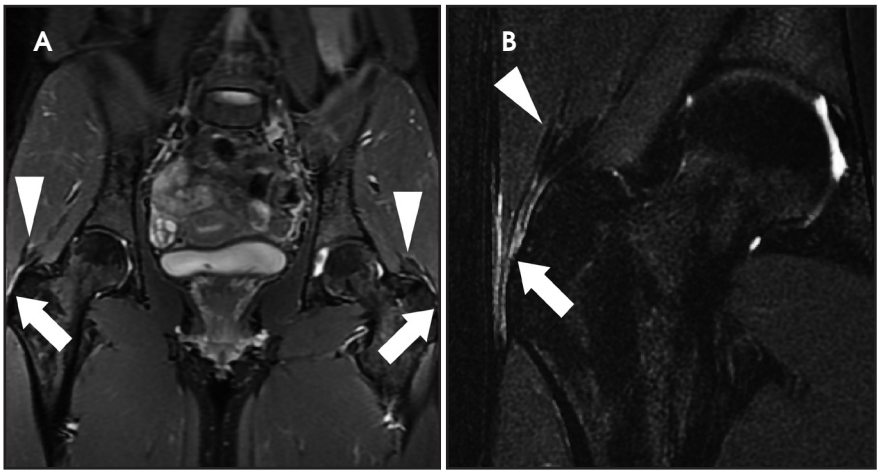

FIGURE 10. *Peritrochanteric edema. Coronal STIR MR image of the pelvis (A) and coronal T2-weighted fat-suppressed image of the right hip (B) in a 25-year-old woman with right hip pain depict increased signal intensity paralleling both the affected and asymptomatic greater trochanters (arrows). There is no fluid distention of the trochanteric bursae and the underlying gluteus medius tendon fibers are intact, thin, and homogeneously hypointense (arrowheads). This imaging appearance is compatible with peritrochanteric edema without findings of gluteal tendinopathy, tendon tear, or trochanteric bursitis. This finding is commonly bilateral, asymptomatic, and seen in older patients. Note a small amount of fluid within the left subgluteus medius bursa and deep to the right iliotibial band.*

Supraacetabular fossa

The supraacetabular fossa (SAF) is a defect in the subchondral bone at the 12 o'clock position of the acetabular roof, with an incidence in the population of approximately 10%. On average, the SAF is located 8 mm lateral to the acetabular notch in the coronal plane. Though the overlying articular cartilage is intact, its location at the weight-bearing portion of the acetabulum poses a risk for this variant to be incorrectly described as an osteochondral or chondral defect of the acetabular cartilage. It can be differentiated from a pathologic lesion of the acetabulum by its smooth margins, absence of subjacent bone marrow edema, and absence of adjacent cartilage irregularity or signal heterogeneity (Figure 4). The average size of a SAF is 5.2 x 4.5 mm in width and 3 mm in depth.[24] SAF can be either partially or completely filled with cartilage. A SAF filled with cartilage may be arthroscopically occult but may fill with synovial fluid or contrast on MR arthrography.[24,25]

Stellate crease

Another variant of the acetabular roof is the stellate crease, which is typically an arthroscopic finding only. While the SAF is a focal defect of bone, the stellate crease is a focal defect of articular cartilage. It is located more medially within the acetabular roof than the SAF, immediately adjacent to the acetabular notch (Figure 5). It is a thin, star-shaped focal bare area devoid of articular cartilage and can be mistaken for a pathologic defect at MRI and arthroscopy. Its characteristic shape, location, clean margins, and lack of associated bone marrow abnormality help distinguish the stellate crease from a true cartilage abnormality.[21,24,26,27] In addition, acquired cartilage defects should not be limited to just this location.

Synovial herniation pit

A synovial herniation pit, also known as "Pitt's pit," is commonly encountered on radiography as a well-circumscribed round or oval lucency with a surrounding narrow zone of sclerosis located in the subchondral or subcortical anterosuperior femoral neck. On MRI, it demonstrates central T2-weighted hyperintensity with a corresponding low signal intensity rim (Figure 6). These lesions are occasionally associated with marrow edema. Synovial herniation pits are typically less than 1 cm but have been reported to enlarge over time.[28] Pathologically, these lesions are composed of fibrocartilaginous tissue and were originally hypothesized to represent sequelae of extra-articular structures such as the iliopsoas tendon or iliofemoral ligament exerting pressure on the underlying synovium, resulting in herniation of synovium into the underlying bone through a cortical defect.[29] More recently, synovial herniation pits are postulated to represent sequelae of repeated contact between the femoral head-neck junction and acetabulum, supported by at least one study showing a higher incidence in patients with femoroacetabular impingement compared to the normal population (33% versus 5%, respectively).[30] Given the risk of progression to primary osteoarthritis in patients with femoroacetabular impingement, identification of a synovial herniation pit warrants close attention to femoroacetabular morphology.[31]

Soft tissue pitfalls

Iliopsoas bursa

The iliopsoas bursa is located lateral to the femoral artery and vein and deep to the myotendinous portion of the iliopsoas muscle. It is the largest bursa in the body, measuring up to 3 x 6 cm.[32] It is present in most individuals and directly communicates with the hip joint in approximately 15% of cases.[32] When distended with fluid or debris, it assumes a characteristic appearance of one or two ovoid or teardrop shaped collections on either side of the iliopsoas tendon (Figure 7). The bursa travels along with the iliopsoas tendon toward the tendon attachment on the lesser trochanter. The bursa can also extend cephalad into the iliac fossa, where it can become quite large. Though iliopsoas bursitis can be a cause of hip pain, it is important to consider communication between the hip joint and iliopsoas bursa, as a distended or debris-filled bursa may reflect intra-articular pathology rather than bursitis.[33,34] It is also important not to mistake

the bursa for a paralabral cyst, cystic mass, or pelvic lymphadenopathy. It is the authors' experience that paralabral cysts invariably lie lateral to the iliopsoas tendon, whereas bursitis usually starts medial to the tendon or envelops it from both sides.

Obturator externus bursa

The obturator externus bursa is a potential space located between the obturator externus tendon and the ischiofemoral capsular ligaments at the posterior aspect of the hip joint capsule. It communicates with the hip joint in all cases, and is considered by some to represent an articular recess rather than a true bursa.[35,36] On MRI, the obturator externus bursa can be a site where intra-articular bodies and joint fluid collect. MR arthrography can distend the capsule and fill the bursa with contrast (Figure 8); it should not be mistaken for a rent or partial tear of the joint capsule.

Plicae and pectinofoveal fold

Several normal synovial reflections in the hip can be mistaken for intra-articular pathology. The ligamentous plica is located within the acetabular fossa at the acetabular attachment of the ligamentum teres. The neck plica parallels the femoral neck, most commonly along the anterior joint capsule. The labral plica is found at the inferomedial margin of the acetabular labrum. The ligamentous and labral plicae are particularly problematic, since they can mimic tears of the ligamentum teres and acetabular labrum, respectively. Plicae are thin, linear, and smooth, in contrast to the irregular and undulating appearance of a torn ligamentum teres or the triangular or trapezoidal shape of a torn section of labrum. Plicae are considered to be embryonic remnants and are seldom symptomatic unless they become entrapped by or between adjacent structures. The labral plica, due to its proximity to the labrum and transverse ligament, is considered to have the highest potential to produce symptoms.[21,27] In contrast, the pectinofoveal fold has no symptomatic potential. The pectinofoveal fold is a linear thickening of the medial hip joint capsule which contains branches of the retinacular arteries and the medial circumflex femoral artery. It extends inferiorly from the more superomedial joint capsule to its inferior attachment, either on the inferomedial femoral neck or on the joint capsule itself (Figure 9). It can be smooth or irregular, and is present in more than 95% of patients at MR arthrography.[37]

Peritrochanteric edema

Lateral hip pain is a common indication for hip imaging. Along with clinical history and physical examination, MRI can contribute to the diagnosis of "greater trochanteric pain syndrome," which is a cause of lateral hip pain posited to be due to a variety of causes, including peritrochanteric bursitis, external snapping hip, and tears or tendinopathy of the gluteal tendons. Though frank tendon tears and imaging findings of bursitis have been shown to correlate with symptoms of lateral hip pain, the finding of peritrochanteric edema alone, identified as increased T2-weighted signal but not a true fluid collection paralleling the greater trochanter on axial or coronal MR images (Figure 10), does not correlate with hip pain.[38,39] Its frequency increases with patient age and is frequently bilateral. Although gluteal tendinopathy occurs more commonly in women, there is no gender predilection associated with peritrochanteric edema.[39] Peritrochanteric edema is extremely common in patients undergoing hip imaging, and may represent the mildest end of a spectrum of lateral hip pathology at its asymptomatic stage. When it occurs in isolation, particularly bilaterally and in an older patient, it can be relegated to the findings section of a report and should not be used to suggest findings of greater trochanteric pain syndrome.[40]

Summary

Several labral, osteocartilaginous, and soft tissue normal variants exist around the hip joint that may mimic, and must be distinguished from, true pathologic conditions. Awareness of these conditions can prevent unnecessary evaluation or intervention. Additionally, although these entities are typically asymptomatic, some normal variants may herald an underlying process such as abnormal biomechanics, which may predispose the hip to disease. MR arthrography can increase specificity and diagnostic confidence in uncertain cases.

References

1. Potter HG, Schachar J. High resolution noncontrast MRI of the hip. *J Magn Reson Imaging.* 2010;31(2):268-278.
2. Petchprapa CN, Dunham KS, Lattanzi R, et al. Demystifying radial imaging of the hip. *Radiographics.* 2013;33(3):E97-E112.
3. Zlatkin MB, Pevsner D, Sanders TG, et al. Acetabular labral tears and cartilage lesions of the hip: indirect MR arthrographic correlation with arthroscopy--a preliminary study. *AJR Am J Roentgenol.* 2010;194(3):709-714.
4. Petchprapa CN, Rybak LD, Dunham KS, et al. Labral and cartilage abnormalities in young patients with hip pain: accuracy of 3-Tesla indirect MR arthrography. *Skeletal Radiol.* 2015;44(1):97-105.
5. Byrd JW, Jones KS. Diagnostic accuracy of clinical assessment, magnetic resonance imaging, magnetic resonance arthrography, and intra-articular injection in hip arthroscopy patients. *Am J Sports Med.* 2004;32(7):1668-1674.
6. Smith TO, Hilton G, Toms AP, et al. The diagnostic accuracy of acetabular labral tears using magnetic resonance imaging and magnetic resonance arthrography: a meta-analysis. *Eur Radiol.* 2011;21(4):863-874.
7. Ziegert AJ, Blankenbaker DG, De Smet AA, et al. Comparison of standard hip MR arthrographic imaging planes and sequences for detection of arthroscopically proven labral tear. *AJR Am J Roentgenol.* 2009;192(5):1397-1400.
8. Schmid MR, Notzli HP, Zanetti M, et al. Cartilage lesions in the hip: diagnostic effectiveness of MR arthrography. *Radiology.* 2003;226(2):382-386.
9. Mintz DN, Hooper T, Connell D, et al. Magnetic resonance imaging of the hip: detection of labral and chondral abnormalities using noncontrast imaging. *Arthroscopy.* 2005;21(4):385-393.
10. Sutter R, Zubler V, Hoffmann A, et al. Hip MRI: how useful is intraarticular contrast material for evaluating surgically proven lesions of the labrum and articular cartilage? *AJR Am J Roentgenol.* 2014;202(1):160-169.
11. Sundberg TP, Toomayan GA, Major NM. Evaluation of the acetabular labrum at 3.0-T MR imaging compared with 1.5-T MR arthrography: preliminary experience. *Radiology.* 2006;238(2):706-711.
12. Park SY, Park JS, Jin W, et al. Diagnosis of acetabular labral tears: comparison of three-dimensional intermediate-weighted fast spin-echo MR arthrography with two-dimensional MR arthrography at 3.0 T. *Acta Radiol.* 2013;54(1):75-82.

13. Lecouvet FE, Vande Berg BC, Malghem J, et al. MR imaging of the acetabular labrum: variations in 200 asymptomatic hips. *AJR Am J Roentgenol.* 1996;167(4):1025-1028.
14. Aydingoz U, Ozturk MH. MR imaging of the acetabular labrum: a comparative study of both hips in 180 asymptomatic volunteers. *Eur Radiol.* 2001;11(4):567-574.
15. Blankenbaker DG, Tuite MJ. Acetabular labrum. *Magn Reson Imaging Clin N Am.* 2013 ;21(1):21-33.
16. McCarthy JC, Noble PC, Schuck MR, et al. The Otto E. Aufranc Award: The role of labral lesions to development of early degenerative hip disease. *Clin Orthop Relat Res.* 2001(393):25-37.
17. Fitzgerald RH, Jr. Acetabular labrum tears. Diagnosis and treatment. *Clin Orthop Relat Res.* 1995(311):60-68.
18. Lage LA, Patel JV, Villar RN. The acetabular labral tear: an arthroscopic classification. *Arthroscopy.* 1996;12(3):269-272.
19. Saddik D, Troupis J, Tirman P, et al. Prevalence and location of acetabular sublabral sulci at hip arthroscopy with retrospective MRI review. *AJR Am J Roentgenol.* 2006;187(5):W507-511.
20. Magerkurth O, Jacobson JA, Morag Y. Prevalence of the acetabular sublabral sulcus at MR arthrography in patients under 17 years of age: does it exist? *Skeletal Radiol.* 2015;44(7): 953-961.
21. DuBois DF, Omar IM. MR imaging of the hip: normal anatomic variants and imaging pitfalls. *Magn Reson Imaging Clin N Am.* 2010;18(4): 663-674.
22. Arho O. Raajojen ylilukuiset hut röntgenkuvissa. [Accessory bones of extremities in roentgen picture.]. *Duodecim.* 1940(56):399-410.
23. Hergan K, Oser W, Moriggl B. Acetabular ossicles: normal variant or disease entity? *Eur Radiol.* 2000;10(4):624-628.
24. Dietrich TJ, Suter A, Pfirrmann CW, et al. Supraacetabular fossa (pseudodefect of acetabular cartilage): frequency at MR arthrography and comparison of findings at MR arthrography and arthroscopy. *Radiology.* 2012;263(2):484-491.
25. Byrd JW. [Hip arthroscopy. Portal technique and arthroscopic anatomy]. *Orthopade.* 2006;35(1):41-42, 44-50, 52-43.
26. Keene GS, Villar RN. Arthroscopic anatomy of the hip: an in vivo study. *Arthroscopy.* 1994;10(4):392-399.
27. Nguyen MS, Kheyfits V, Giordano BD, et al. Hip anatomic variants that may mimic pathologic entities on MRI: nonlabral variants. *AJR Am J Roentgenol.* 2013;201(3):W401-408.
28. Crabbe JP, Martel W, Matthews LS. Rapid growth of femoral herniation pit. *AJR Am J Roentgenol.* 1992;159(5):1038-1040.
29. Pitt MJ, Graham AR, Shipman JH, et al. Herniation pit of the femoral neck. *AJR Am J Roentgenol.* 1982;138(6):1115-1121.
30. Leunig M, Beck M, Kalhor M, et al. Fibrocystic changes at anterosuperior femoral neck: prevalence in hips with femoroacetabular impingement. *Radiology.* 2005;236(1):237-246.
31. Tannast M, Siebenrock KA, Anderson SE. Femoroacetabular impingement: radiographic diagnosis--what the radiologist should know. *AJR Am J Roentgenol.* 2007;188(6):1540-1552.
32. Varma DG, Richli WR, Charnsangavej C, et al. MR appearance of the distended iliopsoas bursa. *AJR Am J Roentgenol.* 1991;156(5): 1025-1028.
33. Blankenbaker DG, De Smet AA, Keene JS. Sonography of the iliopsoas tendon and injection of the iliopsoas bursa for diagnosis and management of the painful snapping hip. *Skeletal Radiol.* 2006;35(8):565-571.
34. Blankenbaker DG, Tuite MJ. Iliopsoas musculotendinous unit. *Semin Musculoskelet Radiol.* 2008;12(1):13-27.
35. Guerra J, Jr., Armbuster TG, Resnick D, et al. The adult hip: an anatomic study. Part II: the soft-tissue landmarks. *Radiology.* 1978;128(1):11-20.
36. Robinson P, White LM, Agur A, et al. Obturator externus bursa: anatomic origin and MR imaging features of pathologic involvement. *Radiology.* 2003;228(1):230-234.
37. Blankenbaker DG, Davis KW, De Smet AA, et al. MRI appearance of the pectinofoveal fold. *AJR Am J Roentgenol.* 2009;192(1):93-95.
38. Blankenbaker DG, Ullrick SR, Davis KW, et al. Correlation of MRI findings with clinical findings of trochanteric pain syndrome. *Skeletal Radiol.* 2008;37(10):903-909.
39. Haliloglu N, Inceoglu D, Sahin G. Assessment of peritrochanteric high T2 signal depending on the age and gender of the patients. *Eur J Radiol.* 2010;75(1):64-66.
40. Klontzas ME, Karantanas AH. Greater trochanter pain syndrome: a descriptive MR imaging study. *Eur J Radiol.* 2014;83(10):1850-1855.